



2nd International Conference on Structural Integrity, ICSI 2017, 4-7 September 2017, Funchal, Madeira, Portugal

A numerical investigation of the stress intensity factor for a bent chevron notched specimen: Comparison of 2D and 3D solutions

Stanislav SEITL^{a*}, Petr MIARKA^{a,b}, Jakub SOBEK^b, Jan KLUSÁK^a

^a*Institute of Physics of Materials, Academy of Sciences of the Czech Republic, Žitkova 22, 616 62, Czech Republic*

^b*Faculty of Civil Engineering, Brno University of Technology, Veverří 331/95, Brno 602 00, Czech Republic*

Abstract

In the contribution, normalized stress intensity factors for three- and four-point bending specimens with a chevron notch is introduced by varying the chevron notch angle and length. The three- and two-dimensional models of bent chevron notched specimens in the software ANSYS were prepared by using possible symmetrical conditions. The 2D model was used with variable thicknesses of the layers representing the characteristic shape of the chevron notch (with the plane stress boundary condition). The numerically obtained results from the 2D and 3D solutions are compared with data from literature.

© 2017 The Authors. Published by Elsevier B.V.

Peer-review under responsibility of the Scientific Committee of ICSI 2017

Keywords: Fracture mechanics; Calibration curves; Stress intensity factor; Chevron notch;

1. Introduction

Knowledge of fracture mechanics parameters is of major importance in design of structural elements and structures themselves. For evaluation of these properties, the researchers postulated some standards ASTM E1820-16 (2016) recommendations RILEM (1991). For experimental tests, various geometries can be used in dependence on application, e.g. three point (3PBT – Korte et al. 2014) or four point (4PBT) bending tests EN 12390-5 (2009), a wedge splitting test (WSTLinsbauer & Tschegg 1986, Brühwiler et al. 1990, Seitl et al. 2011, Seitl et al. 2014), or a

* Corresponding author. Tel.: +420 532 290 361;

E-mail address: seitl@ipm.cz

combination WST/3PB - Seitl et al. (2014), Seitl & Diego Liedo (2017), a modified compact tension test (MCT - Seitl et al. 2017, Seitl & Viszlay, 2017).

A four-point bending test (4PBT) EN 12390-5 (2009) is a destructive fracture test, used for testing ductile, brittle and quasi-brittle materials. This fracture test was upgraded by adding a chevron notch Calomino (1994) into a normalized cross section. The chevron notch is a V-shape notch usually cut from the bottom to the top of a specimen with various angles, beginnings and endings. By cutting out this type of notch, the so-called stress concentrator was created and the crack could propagate directly in the central plane direction of the tested specimen, because the crack initiates from the sharp tip of the chevron notch – see Fig. 1. A pilot study of using a 2D solution for a chevron notch was published by Sobek et al. in 2018 for 3PB specimens.

The aim of this contribution is to compare stress intensity factor values obtained by using 2D and 3D numerical solutions for chevron notched specimens. To verify the data obtained, the numerical results were compared with the data known from literature Calomino (1994).

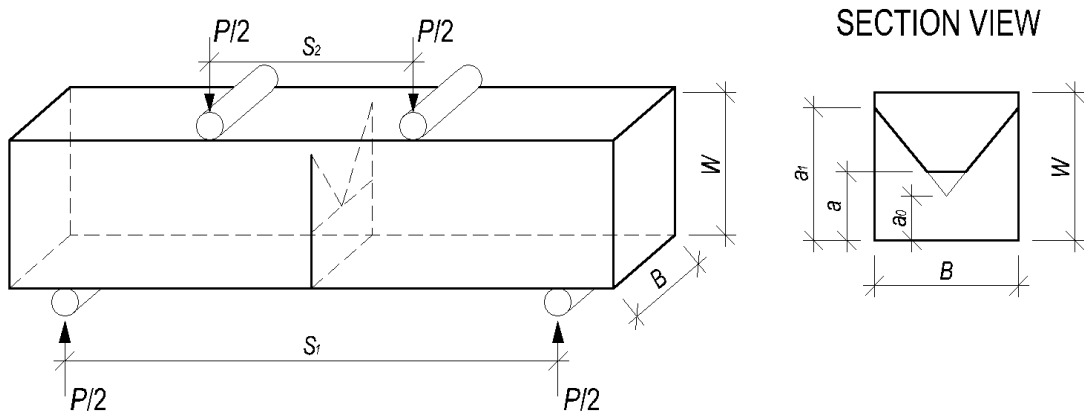


Fig. 1. Studied chevron notched geometry, taken from a NASA report Calomino (1994)

Nomenclature

a	crack length
a_0	chevron notch origin
a_1	chevron notch ending
B	thickness of the specimen
E	Young's modulus
G	shear modulus
K	stress intensity factor
K_I	stress intensity factor in loading mode I
P	loading force
r	polar coordinate – radius
S	span
t	thickness of layer
v	nodal displacement
W	width of the test specimen
Y	calibration curve (shape function)
θ	polar coordinate – angle
κ	Kolosov's constant
ν	Poisson's ratio
σ	applied stress
σ_{ij}	stress tensor component

2. Theoretical Background

The theory used in this contribution is based on linear elastic fracture mechanics. The linear elastic fracture mechanics concept uses the stress field in the close vicinity of the crack tip described by the Williams' expansion Williams (1957). This expansion is an infinite power series originally derived for a homogenous elastic isotropic cracked body, which can be simplified (in the case of loading mode I – tensile loading) into the equation:

$$\sigma_{i,j} = \frac{K_I}{\sqrt{\pi r}} f_{ij}^I(\theta) + O_{ij}(r, \theta), \quad (1)$$

where σ_{ij} represents the stress tensor components, K_I is the stress intensity factor and r, θ are the polar coordinates (provided in the center of the coordinate system at the crack tip; crack faces lie along the x -axis), f_{ij}^I are known shape functions, O_{ij} represent higher order terms.

The value of the stress intensity factor (SIF) for a finite specimen and polar angle $\theta = 0^\circ$ can be expressed in the following form, Anderson (2005):

$$K_I = \sigma \sqrt{\pi a} f(a/W), \quad (2)$$

where σ represents the value of the stress caused by the applied load, a represents the crack length and a/W is the relative crack length. The stress caused by loading in the case of a four-point bending test can be expressed as Karihaloo (1995):

$$\sigma = \frac{PS}{BW^2}, \quad (3)$$

where P is applied loading force, S is the span of the tested specimen, B is the specimen's thickness, W is the specimen's width.

2.1. Calculation Methods

Two different methods were used to calculate the values of the stress intensity factor (SIF). In the 2D solution the KCALC command from the ANSYS software was used, in the 3D the direct method was used.

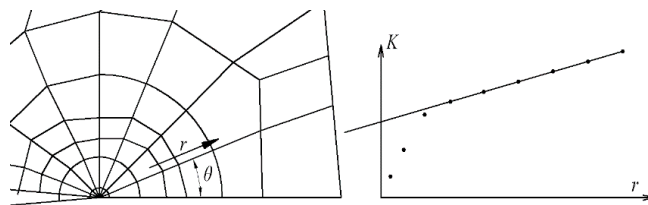


Fig. 2. Extrapolation of the stress intensity factor adopted from Owen & Fawkes (1983)

The KCALC command uses a displacement extrapolation method in the calculation. This method assumes that the displacement calculations are for the plane strain state. The SIF value is then calculated with regard to the symmetrical boundary condition by:

$$K_I = \sqrt{2\pi} \frac{2G}{1+\kappa} \frac{|v|}{\sqrt{r}}, \quad (4)$$

where G is the shear modulus, κ is Kolosov's constant for plane strain or the plane stress condition and r is a radius coordinate in a polar coordinate system, v is nodal displacement.

An extrapolation method (direct method) was used to determinate the values of SIF from 3D numerical calculation. This method is based on stress distribution near the crack tip, and then the value of SIF is extrapolated to the crack tip. The SIF for the crack tip is ascertained from an equation of a usually linear trend line fit through $K(r)$ - values calculated from numerically gained stress values in nodes ahead of the crack, see **Erro! A origem da referência não foi encontrada.**

3. Numerical Modelling

3.1. 3D Numerical Model in ANSYS

A numerical model was created in the finite element (FE) software ANSYS 17.2 [ANSYS® (2016)] as one quarter of the test specimen with symmetrical boundary conditions. The dimensions of $\frac{1}{4}$ of a rectangular prism were span (S) \times width (W) \times thickness (B) 800 mm \times 100 mm \times 100 mm. The geometrical proportions were taken from a NASA report Calomino (1994) meaning the ratio of span/width S/W , the ratio of thickness/width B/W and the load positions, to compare the numerical solution with actual experimental results. The chevron notched cross section was defined with the following parameters: crack length a , chevron notch origin a_0 and chevron notch ending a_1 (Fig. 1). The straight through crack specimen has a relative crack length $\alpha = a/W$. The variants of the chevron notched numerical model have a relative notch length and the surface ($\alpha_1 = a_1/W$), and a relative notch length to the chevron tip $\alpha_0 = a_0/W$ see Fig. 1.

The numerical model was loaded by force $P/2$ which has a magnitude 100 N. Boundary conditions were applied on nodes constraining nodal displacements: $u_x = 0$ in the area which lies on the axis of symmetry, $u_y = 0$ in the ligament area (straight through a crack or chevron notch) and $u_z = 0$ on the line, where the rigid support lies. The geometry and boundary conditions of the numerical model are shown in Fig. 3.

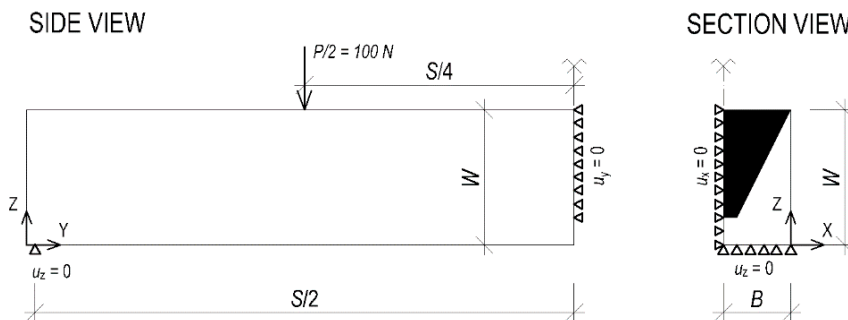


Fig. 3. Boundary conditions of a 3D numerical model

The studied geometry was meshed with the element type SOLID186 taken from ANSYS's element library. In total 8950 elements with 14787 nodes have been used. A fine mesh was adapted around the edge, where the stress was ascertained for the direct calculation of the stress intensity factor (SIF).

The material used in the presented study was Aluminium 7075-T651 with Young's modulus $E = 72.395$ GPa and Poisson's ratio $\nu = 0.3$, taken from the NASA report Calomino (1994).

3.2. Calibration of the 3D model

The 3D numerical model was calibrated, by comparison of 3D and 2D results of SIF obtained from a four-point bending specimen with straight through the crack. The results obtained from the 2D model with plane strain boundary conditions were compared to the results from the direct method conducted on the 3D numerical model with various Poisson's ratios. Calibration was done for a relative crack length $a/W = 0.4$ and Poisson's ratio varied from 0 to 0.499 (numerical calculation is not stable for $\nu = 0.5$), to see the influence of Poisson's ratio on the direct

calculation of the SIF values. The influence is summarized in Tab. 1.

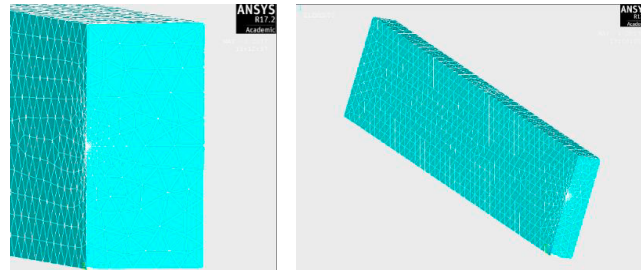


Fig. 4. Meshed numerical model. Right: fine mesh in the middle of the test specimen. Left: axonometric view of the specimen.

The normalized stress intensity factor is transformed into the dimensionless shape function Y , for a four-point bending test specimen by Strawley et al. (1976), Calomino (1994), Knésl et al. (1998), Tada et al. (2000) is determined through Eq.(5).(dependent on the specimen's crack length).

$$Y = \frac{K_I B W^{\frac{3}{2}}}{P(S_1 - S_2)} \quad (5)$$

Table 1. Influence of Poisson's ratio on K_I and the shape function Y , $a/W = 0.4$ – straight through crack specimen

ν [-]	0.0	0.1	0.2	0.3	0.4	0.45	0.499
K_I [MPamm ^{1/2}]	1.4839	1.5081	1.5414	1.6009	1.6886	1.6965	1.6991
$Y_{EQ(5)}$ [-]	1.8549	1.8851	1.9268	2.001	2.1108	2.1206	2.1239

The shape function value for the 2D solution with plane strain boundary conditions is $Y = 2.1235$ for $\nu = 0.5$. The result from plane strain boundary conditions is formally equal to the result from the 3D model (using the direct extrapolation method) with $\nu = 0.5$. The difference in the result with $\nu = 0.499$ and 2D solutions is influenced by a numerical error and by high deviation of the used linear trend line. Comparison of 2D, 3D and the results from literature for 4PB specimens is shown in Fig. 5. The difference between the 2D and 3D solutions is caused by transverse contraction and the influence of dead load.

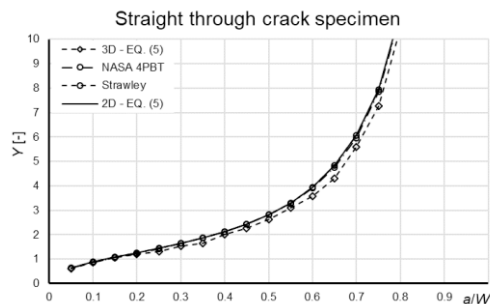


Fig. 5. Comparison of the 3D and 2D models with the shape functions available in literature.

3.3. 2D Numerical Model

Two types of 2D numerical models were conducted by using the FE software ANSYS 17.2. The dimensions and material properties of the 2D numerical models were the same as in the case of the 3D model. The first one was a basic 2D numerical model with the plane strain condition used for calculation of geometry functions Y and to calibrate the 3D numerical model. This model corresponds to the straight through crack case, where boundary conditions are

shown in Fig. 6. The other one was modeled with plane stress conditions to simulate non-uniform thickness of the notch layer along the height of the cross section Sobek et. al. (2017). Each layer varied in thickness (real characteristic in FE code). In total, 30 layers were used, because it was shown in Sobek et. al. (2018) that solutions with more than 10 layers provide accurate and stable numerical calculation. For illustration, the division of the cross section area into 11 specific layers is shown in Fig. 7.

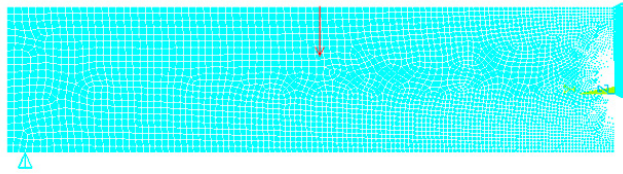


Fig. 6. 2D model with plane strain conditions – applied boundary conditions

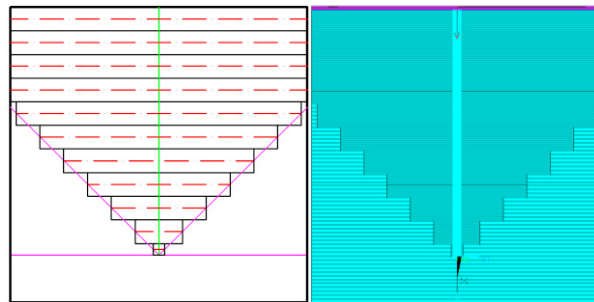


Fig. 7. Cross section area divided into layers. Left: thickness of each layer (red dashed line). Right: numerical model in ANSYS with thicknesses turned on (plane stress condition), including boundary conditions

The element type PLANE82 (8-node element) was used to consider the stress singularity at the crack tip (with the option KSCON). SIF values were calculated by the command KCALC from the ANSYS software. Typical generation of the 2D numerical model is shown in Fig. 8, where the axonometric view is accompanied with the illustration of different thicknesses of layers to simulate the characteristic chevron notched test specimen.

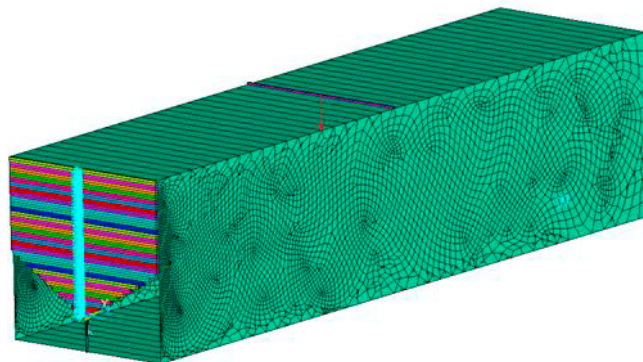


Fig. 8. 2D model with the plane stress condition – axonometric view with plotted element thickness and boundary conditions

4. Numerical results

4.1. Constant Chevron Notch Angle

The SIF values were calculated for various relative crack lengths a/W and with various chevron notch origins a_0/W . The relative crack length varied from 0.05 to 0.95, 0.25 to 0.95 and 0.55 to 0.95 respectively, because of different

initial crack lengths. The numerical results showed a minor difference between 3D and literature Calomino (1994). This difference in numerical results is caused by a transverse contraction. Fig. 9 shows the results for the chevron notch origin $a_0/W = 0.0$ with two different ratios $B/W = 1/2$ and $B/W = 1.0$. The results for the chevron notch origin $a_0/W = 0.2$ and 0.5 with ratio $B/W = 1/2$ can be found in Fig. 10.

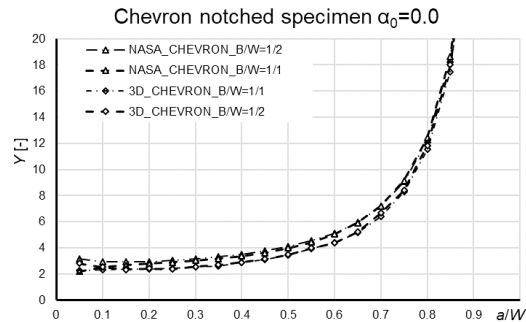


Fig. 9 Comparison of the 3D chevron results with the known literature data $a_0/W = 0.0$ with various B/W ratios.

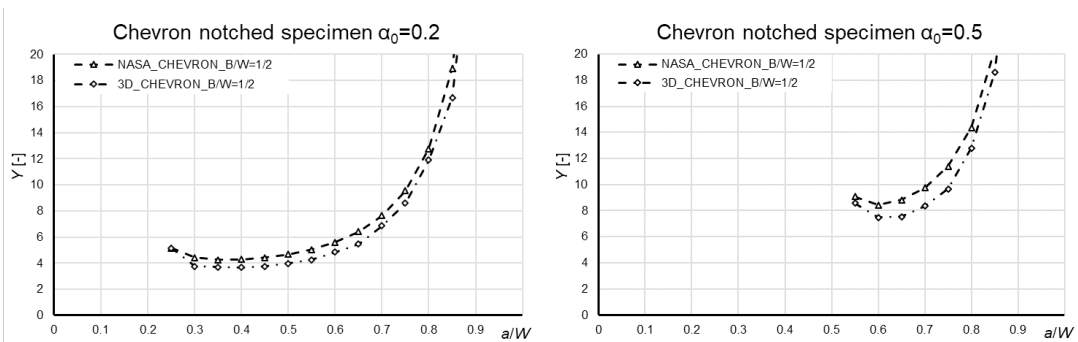


Fig. 10. Comparison of the 3D chevron results with the known literature data $a_0/W = 0.2$ and 0.5 .

4.2. Influence of Angle Changing of a Chevron Notch

The numerical result showed a major difference in the 3D and 2D (non-uniform layer thickness) solutions. To see the influence of the changing of the chevron notch angle on the SIF value three different chevron notch origins were used: $a_0/W = 0.0; 0.2; 0.5$. The chevron notch angle varied by changing the ratio of the chevron notch ending a_1 , with the constant chevron notch origin a_0 . No crack is assumed in these cases. Thus the value $a/W = a_0/W$ for all the configurations. The comparison of the 2D and 3D solutions can be found in Fig. 11.

The differences between the 2D and 3D solutions are influenced by Poisson's ratio effect in 2D and 3D. This effect should not be neglected.

5. Conclusion and Discussion

The numerical study showed good concordance between 3D and the known literature data. This contribution also showed the influence of Poisson's ratio on the SIF calculated from a 3D numerical model. This effect can be seen on both types (Plane strain and Plane stress) of 2D models. However, a 2D model with non-uniform thicknesses showed a major difference from the 3D solution. This effect should be taken into account in cases when the SIF value is calculated using a 3D numerical model.

Acknowledgement

The authors acknowledge the support of Czech Sciences foundation project No.17-01589S.

References

- Anderson, T. L., 2005. Fracture mechanics: Fundamentals and applications. Taylor & Francis group
- ANSYS® 2016. Academic Research, Release 17.2, Help System, Crack analysis guide. Mechanical APDL DocumentationGuide, ANSYS, Inc.
- ASTM E1820-16, 2016. Standard Test Method for Measurement of Fracture Toughness. ASTM international.
- Brühwiler, E., Wittmann, F. H., 1990. The Wedge Splitting Test, a New Method of Performing Stable Fracture Mechanics Test, Engineering Fracture Mechanics 35, p. 117–125.
- Calomino, A., Bubsey, R., Ghosn, L. J. 1994. Compliance Measurements of Chevron Notched Four Point Bend Specimen. NASA Technical Memorandum 106538
- EN 12390-5, 2009. Testing Hardened Concrete –Part 5: Flexural Strength of Test Specimens. European Committee for Standardization.
- Karihaloo, B.L. 1995. Fracture Mechanics and Structural concrete, Longman group limited
- Knésl, Z., Bednář, K., 1998, Two Parameter Fracture Mechanics: Calculation of Parameters and Their Values, IPM AS CR
- Korte, S., Boel, V., De Corte, W., De Schutter, G. 2014 Static and fatigue fracture mechanics properties of self-compacting concrete using three-point bending tests and wedge-splitting tests, Construction and Building Materials 57, p. 1–8
- Linsbauer, H., Tschegg, E., 1986 Fracture energy determination of concrete with cube-shaped specimens, *Zement Beton*, 31, p. 38–40
- Newman, J. C. JR., 1984. A Review of Chevron-notched Fracture Specimens. NASA Technical Memorandum 85797.
- Owen, D. R. J., A. J. Fawkes., 1983. Engineering Fracture Mechanics: Numerical Methods and Applications. Swansea, U.K.: Pineridge Press. ISBN 09-066-7426-3.
- Pook, L. P., 2000. Linear Elastic Fracture Mechanics for Engineers: Theory and Applications. University College London, United Kingdom
- RILEM Report 5, 1991. Fracture Mechanics Test Methods for Concrete Edited by S. P. Shah and A. Carpinteri. Chapman and Hall London.
- Seitl, S., Diego Liedo, R., 2017, Numerical study and pilot evaluation of experimental data on specimen loaded by bending and wedge splitting forces, *Frattura ed Integrità Strutturale*, 11(39), p.100–109.
- Seitl, S., Nieto García, B., Merta I., 2014. Wedge splitting test method: Quantification of influence of glued marble plates by two-parameter fracture mechanics, *Frattura ed Integrità Strutturale*, 30, p. 174–181
- Seitl, S., Korte, S., De Corte, W., Boel, V., Sobek, J., Veselý, V. 2014 Selecting a suitable specimen shape with low constraint value for determination of fracture parameters of cementitious composites, 577–578, p. 481–484
- Seitl, S., Ríos, J.D., Cifuentes, H., Veselý, V. 2017 Effect of the load eccentricity on fracture behavior of cementitious materials subjected to the modified compact tension test, *Solid State Phenomena*, 258 SSP, p. 518–521
- Seitl, S., Vizslay, V., 2017 Modified compact tension specimen for experiments on cement based materials: Comparison of calibration curves from 2D and 3D numerical solutions, *Frattura ed Integrità Strutturale* 11(39) p. 118–128
- Seitl, S., Veselý, V., Routil, L., 2011 Two-parameter fracturemechanical analysis of a near-crack-tip stress field in wedge splitting test specimens, *Computers and Structures* 89(21-22), p. 1852–1858
- Sobek, J., Seitl, S., 2017. Determination of Stress Intensity Factor Value for Chevron-notched Specimen – Pilot Study. Transactions of the VŠB – Technical University of Ostrava, Civil engineering series, Vol. 17, No.1, paper #37 In press
- Sobek, J., Seitl, S., González Menéndez, S., 2018. Numerical Modelling of a Chevron Notched Bend Specimen – Plane Model. Key engineering materials. In press.
- Strawley, J. E., Gross, B., 1976. Side Cracked Plates Subjected to Combined Direct and Bending Forces. Cracks and Fracture ASTM STP 601, pp. 559-579.
- Tada, H., Paris, P. C., Irwin, G. R., 2000. Stress Analysis Handbook, third edition, The American society of mechanical engineering.
- Williams, M. L., 1957. On the Stress Distribution at the Base of a Stationary Crack. ASME J Appl. Mech. Nr. 24, pp. 109–114.

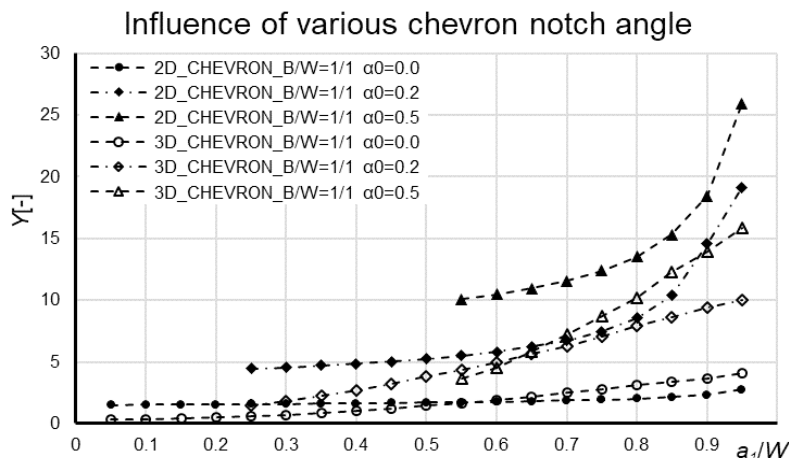


Fig. 11. The influence of the angle changing of a chevron notch on 2D and 3D solutions.